Theory of modal attraction in bimodal birefringent optical fibers

Massimiliano Guasoni,[1,*] Victor V. Kozlov,[2] and Stefan Wabnitz[3]

[1]*Laboratoire Interdisciplinaire Carnot de Bourgogne, UMR 6303 CNRS, Université de Bourgogne, 9 av. Alain Savary, Dijon 21078, France*

[2]*Department of Physics, St.-Petersburg State University, Petrodvoretz, St.-Petersburg 198504, Russia*

[3]*Dipartimento di Ingegneria dell'Informazione, Università degli Studi di Brescia, via Branze 38, Brescia 25123, Italy*

**Corresponding author: massimiliano.guasoni@u-bourgogne.fr*

Received April 9, 2013; revised May 4, 2013; accepted May 7, 2013;
posted May 9, 2013 (Doc. ID 188538); published June 4, 2013

Nonlinear mode coupling among two beams of different wavelength that copropagate in a bimodal highly birefringent optical fiber may lead to the effect of modal attraction. Under such circumstances, the modal distribution of light at a pump wavelength is replicated at the signal wavelength, nearly irrespective of the input mode excitation conditions of the signal. © 2013 Optical Society of America

OCIS codes: (190.4370) Nonlinear optics, fibers; (060.4370) Nonlinear optics, fibers; (190.0190) Nonlinear optics.
http://dx.doi.org/10.1364/OL.38.002029

Nonlinear mode coupling in few-mode optical fibers has been studied for a long time [1], and all-optical mode switching was experimentally demonstrated by Pitois *et al.* [2]. Recently there has been a resurgency of interest in this topic, given the potential of few-mode fibers to enhance the capacity of optical transmission systems via spatial multiplexing [3].

In this Letter, we numerically study the copropagation of two beams of different polarizations and wavelengths in a bimodal optical fiber. By supposing that at one wavelength the input beam is split among two different linearly polarized fiber modes, we reveal that cross-phase modulation leads to an unexpected capability of light to self-organize its modal distribution at the other wavelength. In particular, we show that at a specific distance along the fiber the modal distribution of light at one, say, signal wavelength is attracted, irrespectively of the relative excitation of the two modes at the fiber input, to the same fixed input modal distribution that is imposed at the other (pump) wavelength. In analogy with polarization attraction that occurs in the presence of two beams of different wavelength and arbitrary state of polarization (SOP) in a single-mode fiber [4–6], we name the present effect modal attraction.

In our study we consider an elliptical core bimodal fiber: for wavelengths in the range between the cutoff values of even and odd higher-order modes [1,7], such fiber supports the propagation of four linearly polarized $\mathrm{LP}_{n1,x}$ and $\mathrm{LP}_{n1,y}$ ($n=\{0,1\}$) modes, which for brevity we shall denote nx and ny modes, respectively. The input field is provided by a x-polarized CW pump at frequency ω_p and an orthogonal y-polarized signal at ω_s. All beams copropagate in the fiber along the z direction. $U_n(z)$ ($V_n(z)$) is the complex amplitude of the nx (ny) mode. In the presence of Kerr nonlinearity, one obtains, for the modal amplitudes at the pump frequency,

$$i\dot{U}_n=\frac{2}{3}C_{01}U_mV_nV_m^*\exp(i\Delta\beta_n^u z)+C_{nn}\left(|U_n|^2+\frac{2}{3}|V_n|^2\right)U_n+C_{01}\left(2|U_m|^2+\frac{2}{3}|V_m|^2\right)U_n, \quad (1)$$

where we neglected all nonlinear terms whose phase-matching condition cannot be achieved in practice. In Eq. (1) the dot denotes the z-derivative, and $(n,m)=\{0,1\}$, $m\neq n$. Moreover, $\Delta\beta_0^u\equiv\beta_{1x}(\omega_p)+\beta_{0y}(\omega_s)-\beta_{1y}(\omega_s)-\beta_{0x}(\omega_p)=-\Delta\beta_1^u$ is a wave-vector mismatch, and $\beta_{na}(\omega_f)$ is the propagation constant of the na ($a=\{x,y\}$) mode at frequency ω_f ($f=\{p,s\}$). The equations for signal mode envelopes V_n are simply obtained from Eq. (1) by interchanging the U and V amplitudes and considering that $\Delta\beta_n^v=-\Delta\beta_n^u$.

In Eq. (1) $C_{nn}=n_2\omega/(cA_{nn})$ and $C_{01}=n_2\omega/(cA_{01})$ are the nonlinear fiber coefficients, where $n_2=3.2\cdot10^{-16}$ cm^2/W is the nonlinear index, c is the speed of light in vacuum, $A_{nn}=(\int_{xy}M_n^2\partial x\partial y)^2/(\int_{xy}M_n^4\partial x\partial y)$ is the intramodal effective area of the na modes, and $A_{01}=(\int_{xy}M_0^2\partial x\partial y)(\int_{xy}M_1^2\partial x\partial y)/(\int_{xy}M_0^2M_1^2\partial x\partial y)$ is the intermodal effective area involving the LP_{01} and LP_{11} modes, whose transverse profiles $M_0(x,y)$ and $M_1(x,y)$ are practically polarization independent. Moreover, we assume $\omega_p\approx\omega_s$; hence we only considered $\omega\equiv(\omega_p+\omega_s)/2$ in the nonlinear coefficients. The first term on the right-hand side of Eq. (1) is responsible for modal energy exchanges, and it is not phase matched whenever $|\Delta\beta_n^u|L_{\mathrm{NL}}\gg1$, where $L_{\mathrm{NL}}=1/(C_{00}P)$ is the nonlinear length, and $P\equiv(P_0+S_0)/2$ with P_0 and S_0 the total power at the pump and signal wavelengths, respectively. In the absence of phase matching the magnitudes of the modal amplitudes are preserved, i.e., $|\dot{U}_n|^2=|\dot{V}_n|^2=0$.

For describing modal attraction, it proves convenient to introduce a set of nonlinear parameters, say, **P** and **S**, that we call modal Stokes vectors since they are defined in analogy with the usual Stokes parameters that describe the light SOP. The vector $P=[P_1,P_2,P_3]^T$ has components $P_1=U_0U_1^*+U_1U_0^*$, $P_2=-iU_0U_1^*+iU_1U_0^*$, $P_3=|U_0|^2-|U_1|^2$; the vector $\mathbf{S}=[S_1,S_2,S_3]^T$ is similarly obtained by exchanging the U and V labels. Both **P** and **S** conserve their magnitudes $P_0=(P_1^2+P_2^2+P_3^2)^{1/2}=|U_0|^2+|U_1|^2$ and $S_0=(S_1^2+S_2^2+S_3^2)^{1/2}=|V_0|^2+|V_1|^2$ along z. Hence we may define the unitary modal Stokes vectors $\bar{\mathbf{P}}=\mathbf{P}/P_0$ and $\bar{\mathbf{S}}=\mathbf{S}/S_0$ that evolve on the modal Poincaré sphere. By supposing perfect phase matching

(i.e., whenever $|\Delta\beta_n^u|L_{NL} \approx 0$), Eq. (1) can be rewritten in terms of modal Stokes vectors as

$$\dot{\mathbf{P}} = \mathbf{P} \times (AI_1\mathbf{P} + BI_1\mathbf{S} + C_1^p I_1\mathbf{U} + C_2^p I_2\mathbf{S}), \qquad (2)$$

where $A = 2C_{01} - (C_{00} + C_{11})/2$, $B = (2/3)(A - C_{01})$, $C_1^p = (1/2)(C_{11} - C_{00})(P_0 + (2/3)S_0)$, $C_2^p = -(2/3)C_{01}$, $I_1 = \mathrm{diag}(0,0,1)$, $I_2 = \mathrm{diag}(1,1,0)$, and $\mathbf{U} = [0,0,1]^T$. A similar equation is obtained for S after the mutual exchange of the P and S labels in Eq. (2), and setting $C_1^s = (1/2)(C_{11} - C_{00})(S_0 + (2/3)P_0)$, $C_2^s = C_2^p$. Henceforth we consider the dimensionless distance $\xi \equiv z/L_{\mathrm{NL}}$. Since the total pump power P_0 is a conserved quantity, $\bar{P}_3(\xi) = P_3(\xi)/P_0$ describes the pump modal power distribution (MPD) among the $0x$ and $1x$ modes at any z. Similarly, $\bar{S}_3(\xi) = S_3(\xi)/P_0$ defines the signal MPD among the two y-polarized modes. Whenever $\bar{S}_3 = 1$ ($\bar{S}_3 = -1$), all signal power is carried by mode $0y$ (mode $1y$). Otherwise when $\bar{S}_3 = 0$ the signal power is equally distributed among the two LP modes. In full analogy with polarization attraction, where the output signal SOP is attracted toward the input pump SOP, we may introduce the concept of modal attraction: here the signal MPD $\bar{S}_3(\xi)$ is attracted toward the input pump MPD $\bar{P}_3(0)$. As we shall see, modal attraction only occurs at a particular value of the distance z, e.g., for $\xi = \xi_c$, such that $\bar{S}_3(\xi_c) \to \bar{P}_3(0)$ for any value of the input signal MPD $\bar{S}_3(0)$.

In order to identify and quantify the occurrence of modal attraction, we fixed the input pump modal vector $\mathbf{P}(0)$, and numerically solved Eq. (2) for a set of N different input signal mode vectors $\mathbf{S}^{(k)}(0)$ $(1 \le k \le N)$ that are distributed over the modal Poincaré sphere. Next we evaluated the ensemble average signal MPD $\mu(\xi) = \langle \bar{S}_3(\xi) \rangle$ along with its standard deviation $\sigma(\xi) = \langle \bar{S}_3(\xi)^2 - \mu(\xi)^2 \rangle$.

Note that Eq. (2) is invariant upon rotation about the third (i.e., P_3 and S_3) modal axis. As a result, an arbitrary rotation of both the input pump and the signal modal Stokes vectors about this axis simply rotates the output pump and signal modal Stokes vectors by the same amount. Hence, without loss of generality we may fix $P_2(0) = 0$, so that $|\mathbf{P}(0)|$ is fully determined by the value of $P_3(0)$. Note that the condition $\bar{S}_2(0) = \bar{P}_2(0) = 0$ means that the phase difference among the two modal amplitudes at the signal and pump frequencies is either zero or π.

According to the previous definition, complete modal attraction occurs whenever at some distance along the fiber the MPD $\bar{S}_3^{(k)}(\xi)$ of all output signals converges to just one and the same value: in this case, the standard deviation $\sigma(\xi) = 0$. In contrast, no modal attraction occurs whenever the probability density function of the output signal MPD $\bar{S}_3(\xi)$ has uniform distribution between –1 and 1, so that $\sigma = 1/\sqrt{(3)}$. We may thus define the degree of modal attraction (DOMA) as $\mathrm{DOMA}(\xi) = 1 - \sqrt{3}\sigma(\xi)$, so that DOMA = 1 when full modal attraction is achieved, and DOMA = 0 means that there is no modal attraction. Note that the DOMA has a lower bound equal to $\mathrm{DOMA} = 1 - \sqrt{3} < 0$. Such a negative value is obtained whenever the probability density function of $S_3(\xi)$ is a bimodal Bernoulli distribution, where the two MPD values $\bar{S}_3(\xi) = \pm 1$ have equal probability.

Numerical solutions of Eq. (2) show that the signal MPD $\bar{S}_3(\xi)$ exhibits periodic oscillations with distance. Moreover, modal attraction is maximized for equal pump and signal powers (i.e., with $P_0 = S_0$), and whenever $\bar{S}_2(0) = \bar{P}_2(0)$. The corresponding evolutions of $\bar{S}_3(\xi)$ are shown in Fig. 1 for an input pump MPD $\bar{P}_3(0) = 0.2$, and for a set of input signal $\bar{S}_3(0)$ values distributed between –1 and 1. In Fig. 1(a) we have set $C_{01} = C_{11} = 0.1C_{00}$: as can be seen, the MPD values $\bar{S}_3^{(k)}(\xi)(1 \le k \le 9)$ periodically evolve with distance, with a different oscillation period for each trajectory. Modal attraction does not occur here since there is no particular distance where all trajectories coalesce to the same value of $\bar{S}_3$. On the other hand, the periodic modal evolution trajectories in Fig. 1(b) (which is obtained for $C_{01} = 0.2C_{00}$ and $C_{11} = 0.16C_{00}$) exhibit a nearly identical oscillation period. Moreover, at a certain coalescence point, say, $\xi = \xi_c = 21$ along the fiber, one obtains that $\bar{S}_3^{(k)}(\xi_c) \to \bar{P}_3(0)$, which means that full modal attraction is attained. In real units, for $P = 2$ W and $C_{00} = 2$ W^{-1} km^{-1}, one obtains that the distance $\xi = \xi_c = 21$ corresponds to $L = 5.25$ km.

The comparison among the signal MPD evolutions in Figs. 1(a) and 1(b) reveals that modal attraction occurs only as long as the nonlinear cross-coupling coefficient $C_{01} \ge C_{01,c}$, where $C_{01,c}$ is a critical cross-coupling value.

We obtained the nonlinear modal coefficients corresponding to Fig. 1(b) by considering the case of a highly birefringent, elliptical core bimodal fiber with core and cladding refractive indexes equal to 1.450 and 1.445, respectively. The two elliptical core axes are equal to 5.8 and 3 μm. Numerical finite element simulations using COMSOL show that such fiber is truly bimodal in the telecom band from 1480 to 1560 nm. In addition, over this wavelength range the phase matching condition $|\Delta\beta_n^u| = |\Delta\beta_n^v| \approx 0$ is verified for pump–signal wavelength separations of about 3 nm.

In Fig. 2(a) we illustrate some examples of DOMA evolution along the fiber when $C_{01} = 0.2C_{00}$, $C_{11} = 0.16C_{00}$. Here we consider an input set of N=45 signal modal Stokes vectors $\bar{\mathbf{S}}^{(k)}(0)$ which are situated on the meridian circle of the modal Poincaré sphere defined by the condition $S_2 = \bar{P}_2(0) = 0$ [see Fig. 3(a)]. Clearly the corresponding input signal DOMA(0) = 0. As could be expected from the individual signal MPD evolutions of Fig. 1(b), nearly unitary DOMA is achieved whenever $\xi \cong \xi_c = 21$, for most of the input pump MPD $\bar{P}_3(0)$. Note,

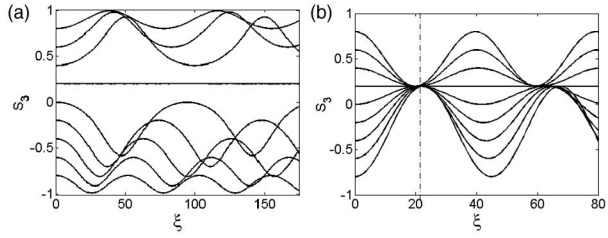

Fig. 1. Evolution with distance ξ of the signal MPD $\bar{S}_3^{(k)}$ for two different sets of nonlinear coefficients. (a) Oscillations have different periods and ranges and (b) oscillations have almost the same period and coalesce at $\xi_c = 21$ as marked by the dotted–dashed vertical line.

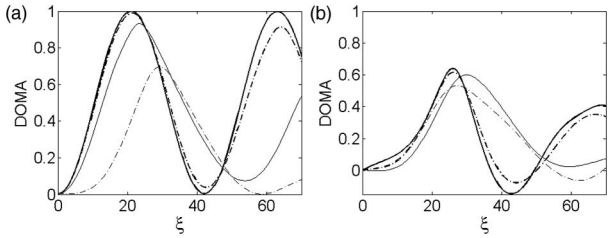

Fig. 2. DOMA versus distance ξ for different input pump modal power distributions: $\bar{P}_3(0) = 0$ (bold line), $\bar{P}_3(0) = \pm 0.2$ (bold dashed–dotted line), $\bar{P}_3(0) = \pm 0.6$ (thin line), and $\bar{P}_3(0) = \pm 1$ (thin dashed–dotted line). (a) The input set of vectors covers the circle $S_2 = 0$ [Fig. 3(a)]. (b) The input set covers the whole sphere [Fig. 4(a)].

however, that a degradation of the signal DOMA is observed whenever $\bar{P}_3(0) \to \pm 1$.

The strength of modal attraction is well illustrated by the plot of Fig. 3(b): here we show all output signal modal Stokes vectors at $\xi = \xi_c$ for the input MPD $\bar{P}_3(0) = 0.2$. All $\bar{S}_3^{(k)}(\xi_c)$ values are found within the range 0.18–0.22, which means that the tips of all output signal modal Stokes vectors are found in a narrow ring centered around the parallel with $S_3 = \bar{P}_{x3}(0) = 0.2$. A similar result is also found for other values of the pump MPD $\bar{P}_3(0)$. Note that in all cases the modal attraction point remains fixed at $\xi_c \approx 21$, where the signal MPD values coalesce toward the input pump MPD.

In their evolution over the modal Poincaré sphere, the tips of the signal modal Stokes vectors from the fiber input $\xi = 0$ [Fig. 3(a)] up to the coalescence point ξ_c [Fig. 3(b)] trace a set of closed trajectories. However unless the input signal Stokes vectors $\bar{\mathbf{S}}^{(k)}(0)$ are arranged on the meridian circle $S_2 = 0$, no single coalescence distance can be found such that their output tips are arranged on a parallel circle with $S_3 = \text{const}$. Therefore, whenever the input set of signal modal Stokes vectors $\bar{S}^{(k)}(0)$ covers the entire modal Poincaré sphere [see Fig. 4(a)], a unitary output DOMA is no longer obtained. This case is illustrated by Fig. 2(b) ($N = 264$): the peak output DOMA $\approx$ 0.65 at $\xi \cong 26$. The tips of the output signal modal Stokes vectors at $\xi = 26$ are shown in Fig. 4(b) for $\bar{P}_3(0) = 0.2$. As can be seen, the overall DOMA is reduced with respect to the example of Fig. 3(b). Nevertheless, significant modal attraction can still be achieved even in this case, since for 90% of the values of the output signal modal Stokes vectors one has $0 \le \bar{S}_3^{(k)}(\xi = 26) \le 0.4$, whereas the average MPD value is $\mu(\xi = 26) \approx \bar{P}_3(0) = 0.2$.

Whenever short signal pulses are used, the robustness of modal attraction in the presence of dispersive effects remains to be assessed. However, for the range of wavelengths that provides two guided modes, their group velocities have similar values in spite of their different phase velocities [7]. Moreover, recent results for

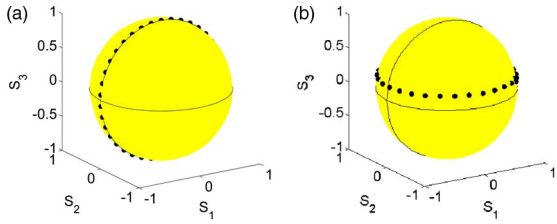

Fig. 3. Poincaré sphere distributions of (a) input and (b) output unitary modal Stokes vectors (black dots) in the case of full modal attraction, $P_0 = S_0$. The input signal modal Stokes lies on the circle $S_2 = 0$. Black horizontal and vertical circles represent $S_3 = 0$ and $S_2 = 0$, respectively.

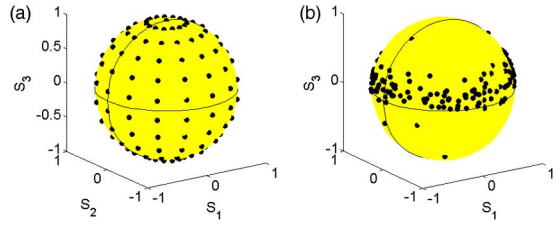

Fig. 4. Poincaré sphere distribution of (a) input and (b) output unitary modal Stokes vectors for the case with modal attraction and $P_0 = S_0$. Here the input signal modal Stokes vectors uniformly covers the sphere.

polarization attraction indicate that modal attraction could even benefit from temporal walk-off between signal pulses and a CW pump [8]. In conclusion, we have shown that, with proper design of the fiber nonlinear coupling coefficients, a beam at a signal wavelength may replicate at the fiber output the relative mode distribution that is imposed at the input pump wavelength, irrespective of the input signal modal content.

This research was funded by the European Research Council under Grant Agreement 306633, ERC PETAL, and by Fondazione Cariplo, grant 2011-0395.

References

1. S. J. Garth and C. Pask, J. Opt. Soc. Am. B **9**, 243 (1992).
2. S. Pitois, A. Picozzi, G. Millot, H. R. Jauslin, and M. Haelterman, Europhys. Lett. **70**, 88 (2005).
3. S. Mumtaz, R. J. Essiambre, and G. P. Agrawal, J. Lightwave Technol. **31**, 398 (2013).
4. J. Fatome, S. Pitois, P. Morin, and G. Millot, Opt. Express **18**, 15311 (2010).
5. V. V. Kozlov, J. Nuño, and S. Wabnitz, J. Opt. Soc. Am. B **28**, 100 (2011).
6. V. V. Kozlov, K. Turitsyn, and S. Wabnitz, Opt. Lett. **36**, 4050 (2011).
7. B. Y. Kim, J. N. Blake, S. Y. Huang, and H. J. Shaw, Opt. Lett. **12**, 729 (1987).
8. V. V. Kozlov, M. Barozzi, A. Vannucci, and S. Wabnitz, J. Opt. Soc. Am. B **30**, 530 (2013).